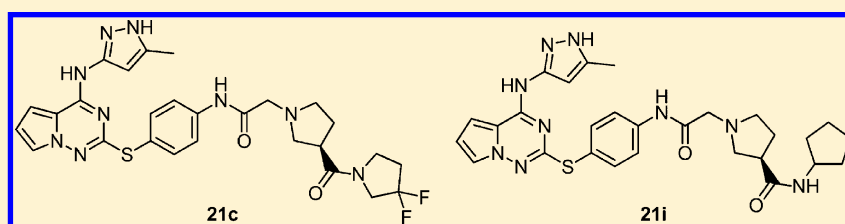


Discovery of Highly Potent and Selective Pan-Aurora Kinase Inhibitors with Enhanced in Vivo Antitumor Therapeutic Index

Gang Liu,^{*,†} Sunny Abraham,[†] Lan Tran,[†] Troy D. Vickers,[†] Shimin Xu,[†] Michael J. Hadd,[†] Sheena Quiambao,[†] Mark W. Holladay,[†] Helen Hua,[‡] Julia M. Ford Pulido,[‡] Ruwanthi N. Gunawardane,[‡] Mindy I. Davis,[§] Shawn R. Eichelberger,[‡] Julius L. Apuy,^{||} Dana Gitnick,^{||} Michael F. Gardner,^{||} Joyce James,^{||} Mike A. Breider,^{||} Barbara Belli,[‡] Robert C. Armstrong,[‡] and Daniel K. Treiber[§]

Departments of [†]Medicinal Chemistry, [‡]Cell Biology and Pharmacology, [§]Technology Development, ^{||}DMPK and Toxicology, and [‡]CMC, Ambit Biosciences Corporation, 4215 Sorrento Valley Boulevard, San Diego, California 92121, United States

S Supporting Information



ABSTRACT: Serine/threonine protein kinases Aurora A, B, and C play essential roles in cell mitosis and cytokinesis. Currently a number of Aurora kinase inhibitors with different isoform selectivities are being evaluated in the clinic. Herein we report the discovery and characterization of **21c** (AC014) and **21i** (AC081), two structurally novel, potent, kinome-selective pan-Aurora inhibitors. In the human colon cancer cell line HCT-116, both compounds potently inhibit histone H3 phosphorylation and cell proliferation while inducing 8N polyploidy. Both compounds administered intravenously on intermittent schedules displayed potent and durable antitumor activity in a nude rat HCT-116 tumor xenograft model and exhibited good in vivo tolerability. Taken together, these data support further development of both **21c** and **21i** as potential therapeutic agents for the treatment of solid tumors and hematological malignancies.

INTRODUCTION

Aurora kinases are a family of three highly homologous serine/threonine kinases that play critical roles during the mitotic stage of the cell cycle.¹ Aurora kinases A and B seem to work in concert during mitosis, whereas the function of Aurora C during mitosis is much less well-defined. Inhibition of Aurora A results in mitotic delay and formation of a monopolar spindle phenotype followed by cell death.² Inhibition of Aurora B results in aberrant endoreduplication and abrogation of cytokinesis, leading to generation of polyploid cells and apoptosis.³ When both Aurora kinases A and B are inhibited, the dominant phenotype is the one resulting from the inhibition of Aurora B.⁴

Both Aurora A and B gene amplification and protein overexpression have been frequently detected in a variety of tumors.⁵ By targeting components of the mitotic machinery, Aurora kinases A and B have been suggested as promising targets for cancer therapy. Intense research over the past decade or so has resulted in more than 10 structurally diverse small-molecule Aurora kinase inhibitors entering early human clinical assessment,⁶ including Aurora A selective 4-((9-chloro-7-(2,6-difluorophenyl)-5H-benzo[*c*]pyrimido[4,5-*e*]azepin-2-yl)-amino)benzoic acid (MLN8054),⁷ Aurora B selective 2-(ethyl(3-(4-(5-(2-(3-fluorophenylamino)-2-oxoethyl)-1H-pyrazol-3-ylamino)quinazolin-7-yloxy)propyl)amino)ethyl dihydro-

gen phosphate (AZD1152),⁸ and pan-Aurora inhibitor N-(4-(((4-((5-methyl-1H-pyrazol-3-yl)amino)-6-(4-methylpiperazin-1-yl)pyrimidin-2-yl)thio)phenyl)cyclopropanecarboxamide (VX-680/MK-0457).⁹

We felt that a pan-Aurora kinase inhibitor may provide more durable efficacy and reduce the chance for the development of resistance driven by target-modifying mutations.¹⁰ Previously, a series of potent pan-Aurora kinase inhibitors with moderate intravenous (iv) clearance was described by this laboratory.¹¹ One such compound (**1**, Figure 1) was found to inhibit tumor growth in a mouse xenograft model using HCT-116 cells when dosed intraperitoneally. However, the significant body-weight loss during the xenograft study complicated the interpretation of the pharmacological effects. In this paper, we describe the further optimization of these pyrrolotriazine-based Aurora kinase inhibitors utilizing a readily accessible, penultimate intermediate **2** (Figure 1), culminating in the discovery of a series of highly potent and kinome selective pan-Aurora kinase inhibitors. Combined with modifications of the in vivo pharmacology protocol, significant tumor growth inhibition and enhanced in vivo tolerability were demonstrated with two lead compounds **21c** and **21i** in a nude rat model.

Received: December 16, 2011

Published: March 1, 2012

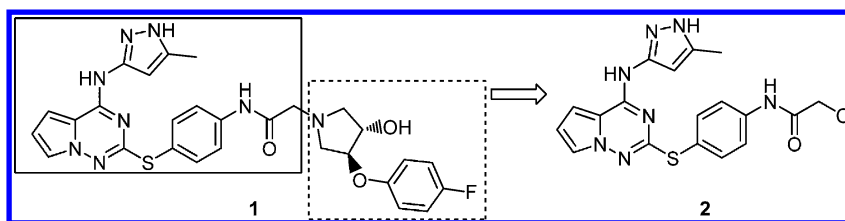
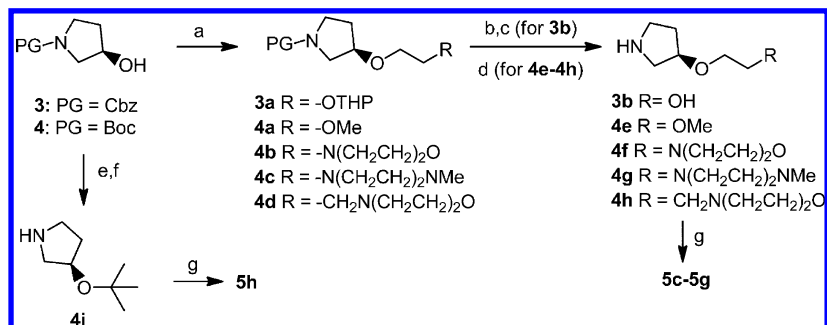


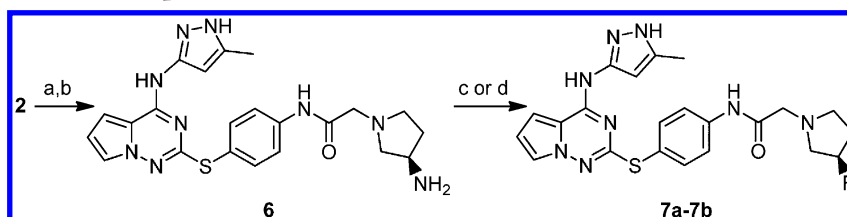
Figure 1. Early lead of pyrrolotriazine-based pan-Aurora inhibitor **1** and a penultimate intermediate **2**.

Scheme 1. General Synthesis of Compounds **5c–h**^a



^aReagents and conditions: (a) NaH, DMF, alkyl halides, 0 °C to rt; (b) 10% Pd/C, H₂, MeOH, rt; (c) aq HCl, THF, rt; (d) 4 N HCl in 1,4-dioxane, rt; (e) *tert*-butyl-2,2,2-trichloroacetimidate, THF, rt; (f) cat. Pd(OH)₂, H₂, MeOH/THF, rt; (g) **2**, KI, *i*-Pr₂NEt, DMF, 50 °C.

Scheme 2. General Synthesis of Compounds **7a,b**^a



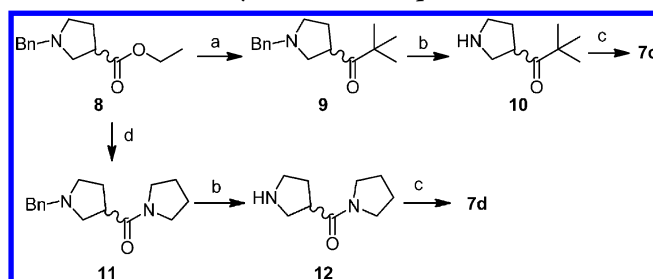
^aReagents and conditions: (a) (*R*)-*tert*-butyl pyrrolidin-3-ylcarbamate, KI, *i*-Pr₂NEt, DMF, 50 °C; (b) 4 N HCl in 1,4-dioxane, rt; (c) *i*-PrCOCl, Et₃N, THF; (d) CH₃SO₂Cl, Et₃N, THF.

CHEMISTRY

The analogues described herein could be prepared in a straightforward fashion via alkylation of the previously described α -chloroacetamide **2**¹² with appropriate pyrrolidine derivatives. Schemes 1 and 3 – 5 illustrate the methods for preparation of a variety of requisite pyrrolidine derivatives prior to reaction with **2**, whereas Scheme 2 illustrates modification of pyrrolidine functionality following reaction with **2**. As shown in Scheme 1, a suitably protected (*R*)-3-hydroxypyrrolidine **3** was subjected to alkylation with various electrophiles to give the corresponding ethers (**3a**, **4a–d**). Removal of the protecting groups resulted in the desired pyrrolidine derivatives (**3b**, **4e–h**). Alkylation of the chloride **2** using these pyrrolidines yielded the desired analogues **5c–g**. Similarly, the formation of the *tert*-butyl ester from **4** followed by hydrogenolysis and alkylation provided compound **5h**.

Scheme 2 demonstrates the facile synthesis of amine **6** followed by acylation or sulfonylation to afford compounds **7a,b**. In Scheme 3, simple transformations of the racemic pyrrolidine carboxylate **8** generated pyrrolidine derivatives **10** and **12** for the syntheses of analogues **7c** and **7d**. In Scheme 4, transformation of 3-pyrrolidinol **13** to *tert*-butyl thioether **14** and subsequent oxidation and deprotection created the pyrrolidine derivatives **15–17**, which were advanced to analogues **7e–g**.

Scheme 3. General Synthesis of Compounds **7c–d**^a

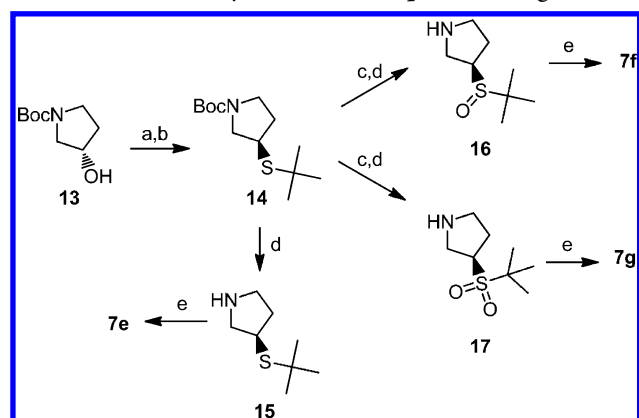


^aReagents and conditions: (a) *t*-BuLi, THF, −78 °C to rt; (b) 10% Pd/C, H₂, MeOH; (c) **2**, KI, *i*-Pr₂NEt, DMF, 50 °C; (d) pyrrolidine, 130 °C, 24 h.

Pyrrolidine carboxamides **21b–l** can be prepared from the enantiomerically pure *N*-Boc β -proline **18**, as shown in Scheme 5. Condensation of the acid with appropriate amines yielded the β -proline carboxamides **19b–l**, which were treated with acid to reveal pyrrolidines **20b–l** for the subsequent alkylation.

RESULTS AND DISCUSSION

The compounds described herein were tested for their binding affinity to the catalytic domain of Aurora kinases A and B in a competition binding assay with an ATP-competitive Aurora

Scheme 4. General Synthesis of Compounds 7e–g^a

^aReagents and conditions: (a) MsCl , TEA, THF, rt; (b) $t\text{-BuSH}$, NaH, DMF, 0 °C to rt; (c) 3-chloroperbenzoic acid, DCM, –30 to –20 °C; (d) 4.5 N HCl in EtOAc/MeOH, 0 °C to rt; (e) **2**, KI, $i\text{-Pr}_2\text{NEt}$, DMF, 50 °C.

inhibitor bound to a solid surface.¹³ The cellular activities of the compounds were assessed in HCT-116 (human colon carcinoma) cells in two formats, measuring either the inhibition of histone H3 phosphorylation (pHH3) mediated by Aurora kinase B¹⁴ or the inhibition of cell proliferation. The compounds described herein were also monitored for their kinase selectivity in a panel of either 321 or 359 distinct kinase domains (not counting mutant variants) using the KinomeScan technology.^{15,16}

As demonstrated by lead compound **1** (Figure 1), the pyrrolo[1,2-*b*]triazine core substituted with an aminopyrazole group at the 4-position and an amidophenylthio group at the 2-position (solid box) constituted a basic pharmacophore for achieving high binding affinity and cell activity. The moderately basic pyrrolidine nitrogen, the pH value of which is attenuated by the anilide carbonyl group, provided an opportunity for ionization and improved aqueous solubility as well as expanded synthetic accessibility.

It is apparent that the structural requirements for the pyrrolidine portion (dashed box) of **1** are not particularly stringent with respect to direct interactions with the enzyme. X-ray structure of the original hit of this series¹¹ in complex with Aurora A kinase was used as the basis for molecular modeling. Docking of a compound (similar to **1**) described previously¹¹ in Aurora A revealed that the pyrrolidine ring was located in an unexplored region flanked by the activation loop and the P loop.¹⁷ It also suggested the possibility of reaching a solvent exposed space through the gap between these two loops. Therefore, we focused on optimizing this pyrrolidine motif with the goal of improving cell potency, pharmacokinetics (PK), and aqueous solubility for intravenous (iv) administration.

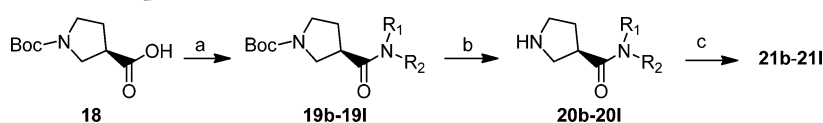
Given the latitude that we had with substituent variations at both the 3- and 4-positions of pyrrolidine ring as described

previously,¹¹ we decided to seek analogues with alternative, simplified pyrrolidine substituents. 3-Monosubstituted pyrrolidines, instead of the 3,4-disubstituted ones, became the focus of the SAR campaign to allow quicker access to structural variations. As shown in Table 1, deleting the 4-fluorophenoxy group of racemic **1** resulted in two enantiomers (**5a**, **5b**) with biological data showing a mild stereochemistry preference in favor of the (*R*)-enantiomer. The decrease in cell activity was particularly notable with the (*S*)-enantiomer **5a**. Therefore, the ensuing analogues were pursued with a primary focus on the (*R*) absolute stereochemistry.

The (*R*)-3-pyrrolidinol was used as a stepping stone for accessing ether analogues with neutral or basic hydrophilic termini, a commonly used SAR maneuver in kinase inhibitor design. Neutral ethers **5c,d** showed marked improvement in cell potency, with methoxyethyl ether analogue **5d** exhibiting more than 10-fold improvement in both cellular assays compared to **5b**. The corresponding kinome selectivity as measured by selectivity score deteriorated slightly for these two compounds. On the other hand, the ether analogues with terminal basic groups (**5e–g**) exhibited weaker cell potency than **5d**, regardless the length of the linker or the basicity of the amino groups. Similar to **5d**, the hydrophobic *tert*-butyl ether analogue **5h** possessed high binding affinity and potent cellular activity. The kinome selectivity of basic analogues **5e–g** was substantially better than the neutral analogues **5a–d** and **5h**.

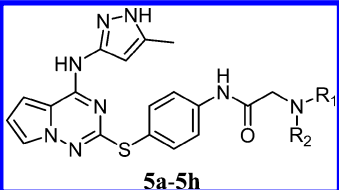
Alternatives to the ether linker at the 3-position of the pyrrolidine ring were also explored. Initial amide and sulfonamide analogues (**7a**, **7b**) resulted in moderately active compounds versus HCT-116 cell proliferation, whereas kinome selectivity was substantially improved (Table 2). We then switched to either a carbon or sulfur-based linker. *tert*-Butyl ketone analogue **7c** possessed encouraging cellular activity, while racemic pyrrolidine amide compound **7d** was even more potent in cells. A diastereomeric mixture of *tert*-butyl sulfoxides (**7f**) exhibited similar cellular activity to **7d** with slightly improved kinome selectivity. The corresponding sulfide **7e** and sulfone **7g** were somewhat less active in cell assays. Encouraged by the excellent *in vitro* profile of compound **7d** and ease of diversification, we pursued additional 3-carboxamide-substituted pyrrolidine derivatives to further define the stereochemistry preference and to fine-tune the suitability for iv formulation.

Even though two enantiomers of pyrrolidine amides (**21a,b**) had very similar binding affinities for Aurora kinases and similar overall kinome selectivity (Table 3), the (*R*)-enantiomer **21b** was ~6-fold more potent in the cellular assays, consistent with the previously observed stereochemistry preference. Further exploration of the tertiary carboxamides (**21c–e**) yielded a series of highly potent compounds against HCT-116 cell proliferation with reasonable kinome selectivity. The preference for lipophilic groups at the terminus of the carboxamide was evident, since the 4-hydroxypiperidine derivative **21f** exhibited a

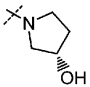
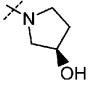
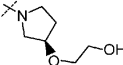
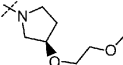
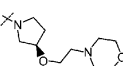
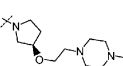
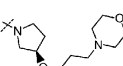
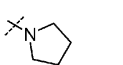
Scheme 5. General Synthesis of Compounds 21b–1^a

^aReagents and conditions: (a) HNR_1R_2 , *O*-(benzotriazol-1-yl)-*N,N,N',N'*-tetramethyluronium tetrafluoroborate (TBTU), Et_3N , DMF, rt; (b) 4 N HCl in 1,4-dioxane, rt; (c) **2**, KI, $\text{NEt-}i\text{-Pr}_2$, DMF, 85 °C.

Table 1. SAR of Monosubstituted Pyrrolidine Derivatives



5a-5h

Compd	NR ₁ R ₂	Aurora A <i>K_d</i> ^a (nM)	Aurora B <i>K_d</i> ^a (nM)	pHH3 <i>IC</i> ₅₀ ^{a,b} (nM)	HCT-116 <i>IC</i> ₅₀ ^{a,c} (nM)	Selectivity Score S(10)
1		15	8	44	5	0.25 ^d
5a		39	14.8	420	227	0.18 ^d
5b		10.5	6.6	103	74	0.21 ^d
5c		4.5	1.7	13	5	0.28 ^d
5d		11.5	3.1	6.2	3.1	0.29 ^d
5e		11	6.6	43.4	17.8	0.15 ^d
5f		12.5	2.9	169	29.8	0.10 ^d
5g		5.1	3.7	27.1	10.8	0.11 ^d
5h		25	3.6	8.9	2.6	0.25 ^d

^aEach experiment was run in duplicate, and the values shown are the average of the two. ^b*IC*₅₀ values are for inhibiting the phosphorylation of histone H3 in the HCT-116 cells. ^c*IC*₅₀ values are for inhibiting the proliferation of HCT-116 cells. ^dThe fraction of 321 kinases having <10% residual activity in the presence of 10 μM inhibitor.

large drop in cell potency despite good binding affinity, perhaps due to compromised cell permeability. Among the large number of secondary amides prepared, many were extremely potent in inhibiting HCT-116 cell proliferation, as exemplified by analogues **21h–l**. Those possessing more hydrophilic amide moieties, such as **21g**, represented the main exceptions.

Some selected analogues were also evaluated in a cellular Aurora A autophosphorylation assay in HEK-293 cells using phosphor antibody readout.¹⁸ Consistent with the high binding affinity for Aurora kinase A, compounds **21c** and **21i** potently inhibited the formation of pAURKA with *IC*₅₀ values of 1 and 2 nM, respectively.

Pharmacokinetics. Since quite a few analogues described herein had very similar in vitro profiles, we used exploratory PK assessments following iv administration to Sprague–Dawley

(SD) rats as a screening assay to further prioritize compounds. Many compounds selected for PK assessment showed high clearance following 1 mg/kg iv bolus dosing. For example, the clearance values (CL) in SD rats for compounds **5d**, **21k**, and **21l** are 62, 48, and 35 mL min^{−1} kg^{−1}, respectively. Compounds **21c** and **21i** exhibited moderate clearance following iv dosing (Table 4) and, taken together with their favorable biochemical and cellular profiles, were selected for further evaluation. The mesylate salts of **21c** and **21i** could be formulated at concentrations greater than 5 mg/mL at pH ≈ 5, using a mixed vehicle TPPW (2% Tween-80, 5% propylene glycol, 10% PG-400, 83% water) suitable for iv dosing in the xenograft models. In athymic nude rats, both compounds exhibited moderate clearance and dose-dependent increase in exposure

Table 2. SAR of Alternative Linkers of the Pyrrolidine Ring

		7a-7b, 7e-7g		7c-7d		
Compd	R	Aurora A	Aurora B	pHH3	HCT-116	Selectivity
		K_d^a (nM)	K_d^a (nM)	$IC_{50}^{a,b}$ (nM)	$IC_{50}^{a,c}$ (nM)	Score S(10)
7a		13.1	5.7	114	46.5	0.12 ^e
7b		12.3	3.2	362	270	0.14 ^e
7c		16.9	6.1	44.8	12.5	0.22 ^e
7d		8.8	2.4	9.0	2.9	0.23 ^e
7e		25.2	14.2	94.5	19.3	0.18 ^e
7f ^d		2.8	3.1	11.9	3.4	0.19 ^f
7g		4.0	4.3	28.6	9.2	0.13 ^f

^aEach experiment was run in duplicate, and the values shown are the average of the two. ^b IC_{50} values are for inhibiting the phosphorylation of histone H3 in the HCT-116 cells. ^c IC_{50} values are for inhibiting the proliferation of HCT-116 cells. ^dA mixture of diastereomers. ^eThe fraction of 321 kinases having <10% residual activity in the presence of 10 μ M inhibitor. ^fThe fraction of 359 kinases having <10% residual activity in the presence of 10 μ M inhibitor.

following iv injection formulated in TPPW, as shown in Table 4.

Cellular Mechanistic Study. Aurora kinase B is essential for chromatin remodeling and cytokinesis. Studies using both pharmacological and genetic disruption of Aurora kinase B in cells led to polyploid cells and loss of viability due to cytokinesis failure.¹⁹ In HCT-116 cells treated with either **21c** and **21i**, 8N polyploidy was potently induced in a dose-dependent manner, with EC_{50} of 3 nM. The observed phenotype was consistent with the IC_{50} values derived from the pHH3 assay and supported the potent Aurora kinase B inhibition in HCT-116 cells by **21c** and **21i**.

Efficacy in Tumor Xenograft Model. On the basis of our experience with compound **1** in a mouse xenograft tumor model¹¹ and literature reports related to Aurora inhibitor in vivo evaluations,²⁰ we were keenly aware of the needs for flexible dosing schedules and drug holidays associated with many Aurora inhibitors. Earlier maximum tolerated dose (MTD) studies in nude rats using **21i** had established that an intermittent dosing schedule was necessary for achieving reasonable tolerability (data not shown). Therefore, two different dosing schedules were selected for evaluating the efficacy and tolerability of **21c** and **21i** as single agents in a subcutaneous flank-tumor xenograft model in nude rats using the HCT-116 cell line: QOD (every other day) for 3 weeks and QD \times 4/week (4 days on and 3 days off per week) for 3 weeks. The data from the QOD schedule are summarized below.

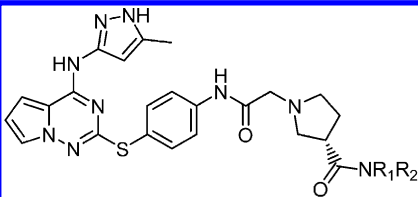
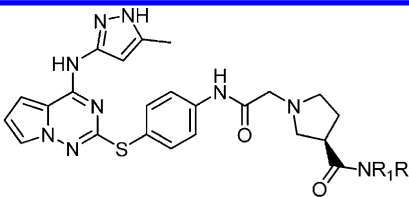
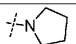
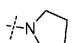
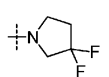
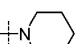
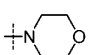
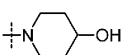
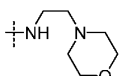
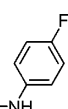
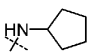
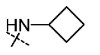
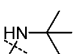
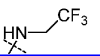
Compound **21c** was dosed as iv bolus every Monday, Wednesday, and Friday over the course of three 7-day cycles. After the dosing was stopped, the animals were observed for 23 additional days. Dose-dependent tumor growth inhibition was observed for all three dosing groups (5, 10, and 20 mpk) (Figure 2). Tumor stasis was observed for the 20 mg/kg dosing group, and it persisted for more than 20 days after dosing. At the end of the study (day 42), 2 out of 10 animals from the 20 mg/kg group were observed with complete regression (CR). Tumor growth inhibition (TGI)²¹ was calculated at 45%, 60%, and 85% for the 5, 10, and 20 mg/kg groups, respectively.

In contrast, the positive control (irinotecan, 100 mg/kg, ip, once per week for 3 weeks) group showed efficacy somewhat less than that of **21c** at 10 mg/kg.

Compound **21i** was evaluated using the same protocol at three doses (10, 20, and 40 mpk). Tumor stasis was observed for the dosing groups at 10 and 20 mg/kg and persisted for more than 40 days after dosing (Figure 3). At the end of the study (day 60), 2 animals (out of 10) with CR for the 10 mg/kg group and 1 CR (out of 10) for the 20 mg/kg group were observed. TGI was calculated at 77% and 82% for the 10 and 20 mg/kg groups, respectively. Doses at 40 mg/kg were not well tolerated, with greater than 10% body weight loss observed (data not shown).

Neither body weight loss nor lethality was noted for either compound at efficacious doses up to 20 mg/kg QOD for 3 weeks. QD \times 4/week schedule also produced favorable signal of

Table 3. SAR of 3-Carboxamide Pyrrolidine Derivatives

						
21a		21b-21l				
Compd	NR ₁ R ₂	Aurora A K _d ^a (nM)	Aurora B K _d ^a (nM)	pHH3 IC ₅₀ ^{a,b} (nM)	HCT-116 IC ₅₀ ^{a,c} (nM)	Selectivity Score S(10)
21a		10.1	1.9	37.6	16.7	0.24 ^e
21b		6.3	2.5	6.3	2.2	0.25 ^d
21c (AC014)		5.8	1.7	6.1	1.2	0.29 ^e
21d		6.4	2.9	10.0	3.2	0.32 ^d
21e		4.0	2.6	14.6	3.9	0.20 ^d
21f		4.0	3.7	293	105	0.148 ^e
21g		6.3	2.9	63.2	19	0.19 ^d
21h		19.5	6.9	42.2	3.8	0.30 ^d
21i (AC081)		9.3	1.9	3.0	2.3	0.33 ^e
21j		4.2	3.3	9.3	1.3	0.31 ^e
21k		5.6	3.1	6.2	1.0	0.33 ^e
21l		2.5	2.2	7.0	0.9	0.35 ^e

^aEach experiment was run in duplicate, and the values shown are the average of the two values. ^bIC₅₀ values are for inhibiting the phosphorylation of histone H3 in the HCT-116 cells. ^cIC₅₀ values are for inhibiting the proliferation of HCT-116 cells. ^dThe fraction of 321 kinases having <10% residual activity in the presence of 10 μ M inhibitor. ^eThe fraction of 359 kinases having <10% residual activity in the presence of 10 μ M inhibitor.

tumor growth inhibition and tolerability for both **21c** and **21i**.²² These results indicate that **21c** and **21i** are efficacious compounds in inhibiting HCT-116 tumor growth in nude rats with enhanced therapeutic index, in comparison to the earlier Aurora kinase inhibitor **1**.

Kinome Selectivity Analysis. Moderate kinome selectivity expressed as S(10) scores (29% and 33%, respectively, of the kinases tested showed <10% of control activity) was observed for both **21c** and **21i** when they were screened at 10 μ M (Table 3). At the efficacious doses in the xenograft studies, the total plasma concentrations for both compounds were only

transiently above 10 μ M. Taking into account the highly plasma protein-bound nature (~99% bound) of **21c** and **21i**, the unbound plasma efficacious concentrations for both compounds were estimated to be largely below 100 nM. Compounds **21c** and **21i** were then screened across a panel of 359 kinases at 100 nM inhibitor concentration. This resulted in low selectivity scores S(10) at 100 nM of 0.07 and 0.08 for **21c** or **21i**, respectively, indicating only a small number of kinases these two compounds were interacting with at an efficacious free concentration of 100 nM. By use of 35% of control activity or below at 100 nM inhibitor concentration as the cutoff, 24

Table 4. Intravenous PK of Compounds 21c and 21i in Rats

compd	rat species	dose (mg/kg)	clearance (mL min ⁻¹ kg ⁻¹)	Vd (L/kg)	AUC _(0–inf) (μM·h)	t _{1/2} (h)
21c ^a	SD	1	21.05	7	1.4	17.5
21c ^b	Nu/Nu	5	19.2	0.7	7.7	1.1
21c ^b	Nu/Nu	15	12.5	0.8	34.4	3.7
21c ^b	Nu/Nu	50	5.23	0.62	181.1	2.9
21i ^a	SD	1	16.92	3.49	1.8	9.4
21i ^b	Nu/Nu	3	27.9	1.0	3.2	1.5
21i ^b	Nu/Nu	10	20.7	1.1	14.6	3.8
21i ^b	Nu/Nu	30	14.7	0.84	62.5	3.4

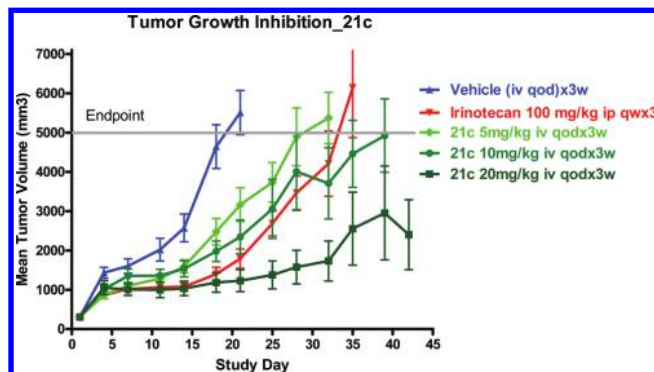
^aVehicle: PEG400/water. ^bVehicle: TPPW.

Figure 2. Efficacy of compound 21c in a Nu/Nu rat tumor xenograft model.

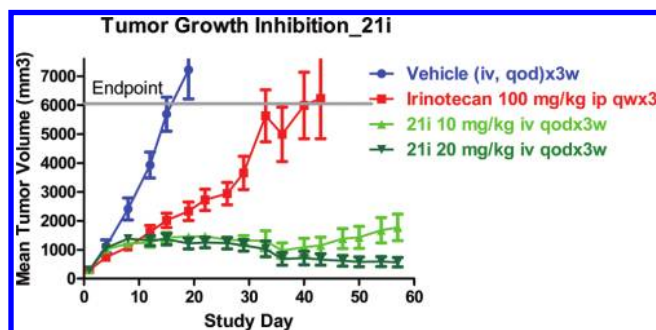


Figure 3. Efficacy of compound 21i in a Nu/Nu rat tumor xenograft model.

and 26 kinases, respectively, for 21c or 21i were picked for the actual binding affinity determination. The complete list and the corresponding K_d values are reported in the Supporting Information.²³ In this analysis, both 21c and 21i were also confirmed to possess high binding affinities for Aurora C, with estimated K_d values of less than 10 nM.

CONCLUSION

Optimization of the lead compound 1 was carried out by installation of carboxamide moieties at the 3-position of the pyrrolidine ring and by removal of the hydroxyl group at the 4-position of the pyrrolidine ring. Compounds 21c (AC014) and 21i (AC081) were identified as highly potent and selective pan-Aurora kinase inhibitors with attractive pharmacokinetic profiles and pharmaceutical properties. Efficacy and enhanced tolerability in nude rat xenograft models were demonstrated with both compounds. Preclinical pharmacology data support clinical development of either or both of these two compounds for the potential treatment of hematological malignancies and solid tumors.

EXPERIMENTAL SECTION

Chemistry. General Methods. Reactions involving air or moisture sensitive reagents were carried out under an argon atmosphere. Proton NMR spectra were obtained in the deuterated solvents indicated on a Bruker Avance 300 or 400, with reference to tetramethylsilane. Routine LC–MS analyses were carried out on a Shimadzu LC–MS 2010 EV system. Reverse phase preparative HPLC purifications were carried out on a Varian preparative HPLC system using a Varian Pursuit XRs diphenyl column as the stationary phase and a mixture of water (5% CH₃CN, 0.05% AcOH) and CH₃CN (0.05% AcOH) as the mobile phase. Chemical purity for all final compounds was determined by analytical HPLC with a C18 column (Phenomenex Luna 5 μm C18(2) 100 Å, 250 mm × 4.6 mm), detected by UV at 254 nm, ELSD, and MS, confirming ≥95% purity.

Syntheses of Representative Compounds (5h, 7a, 7c, 7f, 21c, and 21i) Listed in Tables 1–3. **(R)-3-tert-Butoxypyrrolidine (4i).** To a stirring solution of (R)-(-)-Cbz-3-pyrrolidinol (3) (250 mg, 1.13 mmol) in THF (5 mL) was added *tert*-butyl 2,2,2-trichloroacetimidate (0.20 mL, 1.13 mmol). The solution was stirred at room temperature for 3 h. Then additional *tert*-butyl 2,2,2-trichloroacetimidate (0.20 mL, 1.13 mmol) was added and the mixture was stirred for 0.5 h. Another portion of *tert*-butyl 2,2,2-trichloroacetimidate (0.20 mL, 1.13 mmol) was then added, and the mixture was stirred for an additional 1 h. DCM (15 mL) was then added, and the mixture was filtered through a Celite plug. The filtrate was purified by silica gel chromatography, eluting with 30% EtOAc in hexanes to afford impure (R)-benzyl 3-*tert*-butoxypyrrolidine-1-carboxylate (500 mg). LC–MS (ESI) m/z 300 ($M + Na$)⁺. To the impure (R)-benzyl 3-*tert*-butoxypyrrolidine-1-carboxylate in a mixture of MeOH/THF (1:1, v/v, 8 mL) was added palladium hydroxide (80 mg) and the mixture was stirred under a hydrogen atmosphere overnight, and then filtered through a Celite plug. The filtrate was concentrated under reduced pressure to afford crude (R)-3-*tert*-butoxypyrrolidine (4i) (110 mg, 67%). LC–MS (ESI) m/z 144 ($M + H$)⁺.

(R)-2-(3-*tert*-Butoxypyrrolidin-1-yl)-N-(4-(4-(5-methyl-1H-pyrazol-3-ylamino)pyrrolo[2,1-*f*][1,2,4]triazin-2-yl)thio)phenyl)acetamide Diacetate (5h). General Procedure A. To a stirred mixture of (R)-3-*tert*-butoxypyrrolidine (4i) (69 mg, 0.48 mmol) in DMF (2 mL) were added potassium iodide (40 mg, 0.24 mmol) and 2-chloro-*N*-{4-[4-(5-methyl-1H-pyrazol-3-ylamino)pyrrolo[2,1-*f*][1,2,4]triazin-2-ylsulfanyl]phenyl}acetamide (2) (100 mg, 0.24 mmol), followed by dropwise addition of *N,N*-diisopropylethylamine (0.041 mL, 0.24 mmol). The resulting solution was stirred at 50 °C overnight. Then additional *N,N*-diisopropylethylamine (0.2 mL) and potassium iodide (50 mg) were added and the reaction mixture was stirred at 50 °C for 24 h. The resulting mixture was purified by preparative HPLC to afford (R)-2-(3-*tert*-butoxypyrrolidin-1-yl)-*N*-(4-(4-(5-methyl-1H-pyrazol-3-ylamino)pyrrolo[2,1-*f*][1,2,4]triazin-2-ylthio)phenyl)acetamide as its diacetate salt (5h) (31 mg, 22%). ¹H NMR (300 MHz, methanol-*d*₄) δ 8.03 (d, *J* = 8.5 Hz, 2H), 7.88 (d, *J* = 8.3 Hz, 2H), 7.73 (br s, 1H), 7.20 (d, *J* = 3.2 Hz, 1H), 6.76–6.95 (m, 1H), 6.05 (s, 1H), 4.70 (br s, 1H), 3.95 (br s, 2H), 3.31–3.50 (m, 2H), 3.08–3.22 (m, 1H), 2.52 (td, *J* = 6.9, 13.5 Hz,

1H), 2.40 (s, 3H), 2.24 (s, 6H), 1.54 (br s, 2H), 1.49 (s, 9H). LC–MS (ESI) m/z 521 (M + H)⁺.

(R)-2-(3-Aminopyrrolidin-1-yl)-N-(4-((4-((5-methyl-1H-pyrazol-3-yl)amino)pyrrolo[2,1-f][1,2,4]triazin-2-yl)thio)phenyl)acetamide Dihydrochloride (6). (R)-*tert*-Butyl 1-(2-((4-((5-methyl-1H-pyrazol-3-yl)amino)pyrrolo[2,1-f][1,2,4]triazin-2-yl)thio)phenyl)amino)-2-oxoethylpyrrolidin-3-yl carbamate (prepared using general procedure A from compound 2 and (R)-*tert*-butyl pyrrolidin-3-yl carbamate, 80 mg, 0.14 mmol) was stirred in EtOAc (1.0 mL) at room temperature, and 4 N HCl in 1,4-dioxane (1.0 mL) was added. The resulting mixture was stirred at room temperature for 8 h. Diethyl ether (10 mL) was then added to the mixture, and the precipitate was collected via filtration, washed with diethyl ether, and dried in a vacuum oven to give (R)-2-(3-aminopyrrolidin-1-yl)-N-(4-((4-((5-methyl-1H-pyrazol-3-yl)amino)pyrrolo[2,1-f][1,2,4]triazin-2-yl)thio)phenyl)acetamide dihydrochloride (6) as a white solid (55 mg, 72%). ¹H NMR (300 MHz, DMSO-*d*₆) δ 11.20 (br s, 1H), 10.79–11.05 (m, 1H), 10.70 (br s, 1H), 8.67–8.86 (m, 2H), 8.60 (br s, 1H), 7.77 (d, *J* = 8.3 Hz, 2H), 7.65 (br s, 1H), 7.61 (d, *J* = 7.3 Hz, 2H), 7.23 (br s, 1H), 6.60 (d, *J* = 2.3 Hz, 1H), 5.69 (br s, 1H), 4.47 (d, *J* = 16.4 Hz, 2H), 3.82–4.23 (m, 2H), 3.50–3.81 (m, 2H), 3.38 (d, *J* = 6.2 Hz, 1H), 2.28 (br s, 1H), 2.08 (br s, 3H). LC–MS (ESI) m/z 462 (M – H)⁺.

(R)-N-(1-(2-((4-((4-((5-Methyl-1H-pyrazol-3-yl)amino)pyrrolo[2,1-f][1,2,4]triazin-2-yl)thio)phenyl)amino)-2-oxoethyl)pyrrolidin-3-yl)isobutyramide (7a). General Procedure B. To a suspension of compound 6 (92 mg, 0.17 mmol) in anhydrous THF (2 mL) at 0 °C was added dropwise Et₃N (95 μ L, 0.68 mmol), followed by a solution of isobutyryl chloride (21 μ L, 0.20 mmol) in THF. The reaction mixture was then stirred at room temperature for 2 h. The resulting mixture was quenched with water and extracted by EtOAc (15 mL). The organic layer was separated, dried, and concentrated under reduced pressure. The residue was purified by silica gel chromatography, eluting with DCM in MeOH (20:1 to 10:1, v/v) to give (R)-N-(1-(2-((4-((4-((5-methyl-1H-pyrazol-3-yl)amino)pyrrolo[2,1-f][1,2,4]triazin-2-yl)thio)phenyl)amino)-2-oxoethyl)pyrrolidin-3-yl)isobutyramide (7a) (35 mg, 30% yield). ¹H NMR (400 MHz, DMSO-*d*₆) δ 12.13 (s, 1H), 10.82 (s, 1H), 10.64 (d, *J* = 1.2 Hz, 1H), 10.35 (t, *J* = 1.6 Hz, 1H), 8.15 (d, *J* = 1.2 Hz, 1H), 7.71 (d, *J* = 8.4 Hz, 2H), 7.63 (d, *J* = 8.4 Hz, 2H), 7.57 (s, 1H), 7.21 (q, *J* = 1.2 Hz, 1H), 6.58 (d, *J* = 2.8 Hz, 1H), 5.68 (s, 1H), 4.31 (d, *J* = 2.0 Hz, 2H), 3.30–3.94 (overlapping with solvent, m, 2H), 2.38 (m, 1H), 2.05 (s, 3H), 1.88–1.94 (m, 1H), 1.01 (d, *J* = 6.8 Hz, 6H). LC–MS (ESI) m/z 534 (M + H)⁺.

(1-(1-Benzylpyrrolidin-3-yl)-2,2-dimethylpropan-1-one (9). To a stirred solution of ethyl 1-benzylpyrrolidine-3-carboxylate (400 mg, 1.71 mmol) in THF (5 mL) at –78 °C was added *tert*-butyllithium in THF (1.7 M, 1.0 mL, 1.7 mmol) dropwise. The resulting mixture was left at –78 °C for 30 min before it was allowed to warm to room temperature. After another 90 min, the reaction mixture was quenched with saturated aqueous NH₄Cl (15 mL) and extracted with EtOAc (50 mL). The organic layer was washed with brine (15 mL), dried over Na₂SO₄, and evaporated under reduced pressure. The residue was purified by silica gel column chromatography, eluting with 30–60% EtOAc in hexanes to give (1-(1-benzylpyrrolidin-3-yl)-2,2-dimethylpropan-1-one (9) as a colorless oil (200 mg, 48% yield). ¹H NMR (300 MHz, DMSO-*d*₆) δ 7.32 (d, *J* = 4.0 Hz, 5H), 3.64 (s, 2H), 3.49–3.61 (m, 1H), 2.80–3.02 (m, 2H), 2.29–2.55 (m, 2H), 1.96–2.12 (m, 1H), 1.79–1.95 (m, 1H), 1.12 (s, 9H). LC–MS (ESI) m/z 246 (M + H)⁺.

2,2-Dimethyl-1-(pyrrolidin-3-yl)propan-1-one (10). General Procedure C. Compound 9 (210 mg, 0.86 mmol) was dissolved in 1 mL of MeOH. Then 10% Pd/C (35 mg) was added under argon atmosphere. The mixture was stirred under a hydrogen atmosphere at 60 °C for 2 h. The reaction mixture was then filtered through a Celite plug and the filtrate was evaporated under reduced pressure to give 2,2-dimethyl-1-(pyrrolidin-3-yl)propan-1-one (10) as a colorless oil (120 mg, 90% yield). LC–MS (ESI) m/z 156 (M + H)⁺.

N-(4-((4-((5-Methyl-1H-pyrazol-3-yl)amino)pyrrolo[2,1-f][1,2,4]triazin-2-yl)thio)phenyl)-2-(3-pivaloylpyrrolidin-1-yl)acetamide (7c). Compound 7c was prepared as an off-white solid

(92 mg, 25%) using general procedure A, substituting 2,2-dimethyl-1-(pyrrolidin-3-yl)propan-1-one (10) for pyrrolidine 4i used in general procedure A. ¹H NMR (300 MHz, DMSO-*d*₆) δ 12.08 (br s, 1H), 10.63 (s, 1H), 10.08 (br s, 1H), 7.81 (d, *J* = 8.3 Hz, 2H), 7.52–7.64 (m, 3H), 7.22 (br s, 1H), 6.58 (br s, 1H), 5.63 (s, 1H), 3.56–3.75 (m, 1H), 3.34–3.43 (m, 1H), 3.18–3.30 (m, 1H), 2.91 (t, *J* = 8.6 Hz, 1H), 2.77–2.87 (m, 1H), 2.58–2.67 (m, 1H), 2.56 (br s, 1H), 2.02 (s, 3H), 1.90–2.01 (m, 1H), 1.67–1.86 (m, 1H), 1.10 (s, 9H). LC–MS (ESI) m/z 533 (M + H)⁺.

(R)-tert-Butyl 3-(tert-Butylthio)pyrrolidine-1-carboxylate (14). Step 1. To a stirred solution of (S)-*tert*-butyl 3-hydroxypyrrolidine-1-carboxylate (0.90 g, 4.8 mmol) in THF (5 mL) at 0 °C was added Et₃N (1.39 mL, 10.0 mmol), followed by dropwise addition of methanesulfonyl chloride (0.68 g, 5.8 mmol). The resulting mixture was then stirred at room temperature for 8 h before it was partitioned between EtOAc (50 mL) and water (25 mL). The organic layer was washed with brine (25 mL), dried over MgSO₄, filtered, and concentrated under reduced pressure to give (S)-*tert*-butyl 3-((methylsulfonyl)oxy)pyrrolidine-1-carboxylate (1.07 g, 81%). LC–MS (ESI) m/z 266 (M + H)⁺.

Step 2. To a suspension of NaH (60%, 211 mg, 5.27 mmol) in DMF (3 mL) was added dropwise 2-methylpropane-2-thiol (237 mg, 2.64 mmol) at 0 °C. The reaction mixture was allowed to warm to room temperature and stirred for 20 min. The resulting mixture was added to a solution of (S)-1-(*tert*-butoxycarbonyl)pyrrolidin-3-yl methanesulfonate (350 mg, 1.32 mmol) in DMF (2 mL) at 0 °C. The reaction mixture was stirred at room temperature for 8 h and then quenched with 10% aqueous citric acid solution. The reaction mixture was concentrated under reduced pressure and the residue was purified by flash column chromatography, eluting with 5% EtOAc in petroleum ether to afford (R)-*tert*-butyl 3-(*tert*-butylthio)pyrrolidine-1-carboxylate (14) (300 mg, 88% yield). LC–MS m/z 260 (M + H)⁺.

(R)-3-(tert-Butylsulfinyl)pyrrolidine Hydrochloride (16). Step 1. To a solution of 14 (400 mg, 1.54 mmol) in DCM (5 mL) at –20 °C was added portionwise 70% 3-chloroperbenzoic acid (417 mg, 1.69 mmol). The reaction mixture was stirred at –30 °C for 20 min, then quenched with aqueous Na₂SO₃ (5 mL). The resulting mixture was partitioned between DCM (25 mL) and 10% NaOH (10 mL). The organic layer was washed with brine, dried over Na₂SO₄, filtered, and concentrated under reduced pressure. The residue was purified by flash column chromatography, eluting with 10% EtOAc in dichloromethane to give (R)-*tert*-butyl 3-(*tert*-butylsulfinyl)pyrrolidine-1-carboxylate (220 mg, 52% yield). LC–MS m/z 276 (M + H)⁺.

Step 2. To a solution of (R)-*tert*-butyl 3-(*tert*-butylsulfinyl)pyrrolidine-1-carboxylate (275 mg, 1.00 mmol) in MeOH (2 mL) was added dropwise 4.5 N HCl in EtOAc at 0 °C. The mixture was allowed to warm to room temperature and was stirred for 1 h. The organic solvents were removed under reduced pressure and the residue was dried to afford (R)-3-(*tert*-butylsulfinyl)pyrrolidine hydrochloride (16) (190 mg, 90% yield). LC–MS m/z 176 (M + H)⁺. The crude product was used directly in the next step without further purification.

2-((R)-3-(tert-Butylsulfinyl)pyrrolidin-1-yl)-N-(4-((4-((5-methyl-1H-pyrazol-3-yl)amino)pyrrolo[2,1-f][1,2,4]triazin-2-yl)thio)phenyl)acetamide (7f). Compound 7f was prepared as an off-white solid (22 mg, 21% yield) using general procedure A, substituting (R)-3-(*tert*-butylsulfinyl)pyrrolidine hydrochloride (16) for pyrrolidine 4i used in general procedure A. ¹H NMR (400 MHz, DMSO-*d*₆) δ 12.08 (s, 1H), 10.63 (s, 1H), 10.09 (s, 1H), 7.85 (dd, *J* = 8.0 Hz, 2H), 7.78 (m, 3H), 7.22 (s, 1H), 6.57 (s, 1H), 5.62 (s, 1H), 4.03 (d, *J* = 7.2 Hz, 1H), 3.47 (s, 2H), 3.17–2.64 (m, 4H), 2.32–1.92 (m, 5H), 1.14 (s, 9H). LC–MS m/z 553 (M + H)⁺.

(R)-tert-Butyl 3-(3,3-Difluoropyrrolidine-1-carbonyl)pyrrolidine-1-carboxylate (19c). To a stirred solution of (R)-1-(*tert*-butoxycarbonyl)pyrrolidine-3-carboxylic acid (3.8 g, 17.7 mmol) in DMF (20 mL) were added 3,3-difluoropyrrolidine hydrochloride (2.8 g, 19.5 mmol) and O-(7-azabenzotriazol-1-yl)-N,N,N',N'-tetramethyluronium hexafluorophosphate (8.1 g, 21.3 mmol) sequentially. Triethylamine (7.6 mL, 53.1 mmol) was then slowly added to the reaction mixture. The resulting mixture was then stirred at room temperature overnight. The reaction mixture was quenched with water

(50 mL) and extracted with EtOAc (2 × 50 mL). The combined organic layers were washed with water (25 mL) and brine (25 mL), dried over Na₂SO₄, and evaporated under reduced pressure. The residue was purified by silica gel flash column chromatography, eluting with 0–15% EtOAc in hexanes to give (R)-tert-butyl 3-(3,3-difluoropyrrolidine-1-carbonyl)pyrrolidine-1-carboxylate (**19c**) (4.8 g, 88% yield) as a white solid. ¹H NMR (300 MHz, chloroform-*d*) δ 3.65–3.92 (m, 5H), 3.40–3.64 (m, 3H), 3.34 (br s, 1H), 2.89–3.15 (m, 1H), 2.46 (d, *J* = 5.9 Hz, 1H), 2.29–2.42 (m, 1H), 1.96–2.28 (m, 2H), 1.46 (s, 9H). LC–MS (ESI) *m/z* 305 (M + H)⁺.

(R)-(3,3-Difluoropyrrolidin-1-yl)(pyrrolidin-3-yl)methanone Hydrochloride (20c). To a stirred mixture of **19c** (4.75 g, 15.6 mmol) in EtOAc (10 mL) was added 30 mL of 4 N HCl in 1,4-dioxane. The resulting mixture was stirred at room temperature overnight. The volatile solvents were evaporated under reduced pressure, and the residue was evaporated with CH₃CN (2 × 25 mL). The residue was dried under high vacuum overnight to give (R)-(3,3-difluoropyrrolidin-1-yl)(pyrrolidin-3-yl)methanone hydrochloride **20c** (3.8 g, 100%) as a light yellow thick oil. ¹H NMR (499 MHz, chloroform-*d*) δ 9.96 (br s, 1H), 9.47 (br s, 1H), 3.03–4.70 (m, 6H), 2.13–2.97 (m, 4H), 1.69–2.13 (m, 3H). LC–MS (ESI) *m/z* 205 (M + H)⁺.

(R)-2-(3-(3,3-Difluoropyrrolidine-1-carbonyl)pyrrolidin-1-yl)-N-(4-((4-((5-methyl-1H-pyrazol-3-yl)amino)pyrrolo[2,1-*f*][1,2,4]triazin-2-yl)thio)phenyl)acetamide (21c). General Procedure D. To a stirred solution of compound **2** (6.1 g, 14.8 mmol) in DMF (25 mL) was added compound **20c** (3.8 g, 15.8 mmol) in DMF (10 mL), followed by *N,N*-diisopropylethylamine (6.4 mL, 36.8 mmol) and potassium iodide (0.24 g, 1.4 mmol). The reaction mixture was heated at 85 °C for 4 h. LC–MS indicated the completion of the reaction. The reaction mixture was then cooled to room temperature, quenched with water (50 mL), and extracted with EtOAc (3 × 50 mL). The combined organic layers were washed with water (50 mL) and brine (50 mL), dried over Na₂SO₄, and evaporated under reduced pressure. The residue was purified by silica gel flash column chromatography, eluting with 0–5% MeOH (containing 2 N NH₃)/EtOAc to give (R)-2-(3-(3,3-difluoropyrrolidine-1-carbonyl)pyrrolidin-1-yl)-N-(4-((4-((5-methyl-1H-pyrazol-3-yl)amino)pyrrolo[2,1-*f*][1,2,4]triazin-2-yl)thio)phenyl)acetamide (**21c**) as a white solid (7.1 g, 83% yield). ¹H NMR (300 MHz, DMSO-*d*₆) δ 12.07 (br s, 1H), 10.63 (br s, 1H), 10.13 (br s, 1H), 7.84 (d, *J* = 8.1 Hz, 2H), 7.50–7.76 (m, 3H), 7.23 (br s, 1H), 6.59 (d, *J* = 2.4 Hz, 1H), 5.64 (br s, 1H), 3.97 (t, *J* = 13.0 Hz, 1H), 3.67–3.87 (m, 2H), 3.51–3.66 (m, 2H), 3.06–3.28 (m, 2H), 2.62–3.01 (m, 5H), 2.29–2.47 (m, 1H), 2.12–2.23 (m, 1H), 2.03 (br s, 3H), 1.74–1.96 (m, 1H). LC–MS (ESI) *m/z* 582 (M + H)⁺.

(R)-2-(3-(3,3-Difluoropyrrolidine-1-carbonyl)pyrrolidin-1-yl)-N-(4-((4-((5-methyl-1H-pyrazol-3-yl)amino)pyrrolo[2,1-*f*][1,2,4]triazin-2-yl)thio)phenyl)acetamide Methanesulfonate (21c Mesylate Salt). General Procedure E. To a stirred suspension of compound **21c** free base (7.1 g, 12.2 mmol) in EtOH (40 mL) at room temperature was added methanesulfonic acid (1.23 g, 12.8 mmol) in EtOH (10 mL) dropwise. The resulting mixture was heated at 65 °C, and the reaction mixture became clear soon after the heating was initiated. After heating at 65 °C overnight, the reaction mixture was cooled to room temperature, and Et₂O (20 mL) was added with stirring. The white precipitates were collected via filtration, washed with cold EtOH/Et₂O (1:1, v/v), and dried in a vacuum oven at 50 °C for 1 day to give (R)-2-(3-(3,3-difluoropyrrolidine-1-carbonyl)pyrrolidin-1-yl)-N-(4-((4-((5-methyl-1H-pyrazol-3-yl)amino)pyrrolo[2,1-*f*][1,2,4]triazin-2-yl)thio)phenyl)acetamide methanesulfonate (**6.4 g**, 77%). ¹H NMR (300 MHz, DMSO-*d*₆) δ 12.10 (br s, 1H), 10.82 (br s, 1H), 10.65 (s, 1H), 10.32 (br s, 1H), 7.73 (d, *J* = 8.67 Hz, 2H), 7.64 (d, *J* = 8.67 Hz, 2H), 7.54–7.60 (m, 1H), 7.22 (br s, 1H), 6.59 (dd, *J* = 2.64, 4.33 Hz, 1H), 5.68 (s, 1H), 4.16–4.52 (m, 2H), 3.62–4.10 (m, 4H), 3.08–3.62 (m, 5H), 2.34–2.62 (m, 2H), 2.32 (s, 3H), 1.80–2.21 (m, 4H). LC–MS (ESI) *m/z* 582 (M + H)⁺.

(R)-N-Cyclopentyl-1-(2-((4-((5-methyl-1H-pyrazol-3-yl)amino)pyrrolo[2,1-*f*][1,2,4]triazin-2-yl)thio)phenyl)amino)-2-oxoethylpyrrolidine-3-carboxamide (21i). Compound **21i** (9.4 g, 81% yield) was prepared as a light yellow powder using procedures

analogous to the ones described for the preparation of **21c**, substituting cyclopentylamine for 3,3-difluoropyrrolidine hydrochloride used in the preparation of **19c**. ¹H NMR (300 MHz, DMSO-*d*₆) δ 12.04 (s, 1H), 10.60 (s, 1H), 10.12 (s, 1H), 7.71–7.92 (m, 3H), 7.46–7.65 (m, 3H), 7.21 (br s, 1H), 6.58 (dd, *J* = 2.5, 4.2 Hz, 1H), 5.65 (s, 1H), 4.00 (qd, *J* = 6.9, 13.7 Hz, 1H), 3.37 (s, 1H), 3.21 (d, *J* = 16.2 Hz, 1H), 2.57–2.95 (m, 5H), 2.03 (s, 3H), 1.86–2.00 (m, 2H), 1.78 (d, *J* = 4.3 Hz, 2H), 1.61 (d, *J* = 6.6 Hz, 2H), 1.42–1.55 (m, 2H), 1.36 (dd, *J* = 5.6, 12.0 Hz, 2H). LC–MS (ESI) *m/z* 560 (M + H)⁺.

(R)-N-Cyclopentyl-1-(2-((4-((5-methyl-1H-pyrazol-3-yl)amino)pyrrolo[2,1-*f*][1,2,4]triazin-2-yl)thio)phenyl)amino)-2-oxoethylpyrrolidine-3-carboxamide Methanesulfonate (21i Mesylate Salt). Compound **21i** methanesulfonate (7.4 g, 67%) was prepared as a light yellow powder according to general procedure E, substituting **21i** free base for **21c** free base used in general procedure E. ¹H NMR (300 MHz, DMSO-*d*₆) δ 12.09 (br s, 1H), 10.69–10.87 (m, 1H), 10.65 (s, 1H), 10.27 (br s, 1H), 8.03–8.25 (m, 1H), 7.73 (d, *J* = 8.85 Hz, 2H), 7.64 (d, *J* = 8.85 Hz, 2H), 7.58 (s, 1H), 7.22 (br s, 1H), 6.59 (dd, *J* = 2.64, 4.33 Hz, 1H), 5.68 (br s, 1H), 4.14–4.46 (m, 2H), 3.53–4.09 (m, 3H), 2.98–3.33 (m, 4H), 2.30 (s, 3H), 2.06 (s, 3H), 1.72–1.89 (m, 2H), 1.63 (d, *J* = 6.97 Hz, 2H), 1.46–1.58 (m, 2H), 1.27–1.45 (m, 2H). LC–MS (ESI) *m/z* 560 (M + H)⁺.

Kinase Competition Binding. KinomeScan competition binding assays (www.kinomescan.com) were performed as described previously.¹³

HTC-116 pH3 Cell Assay. HCT-116 cells derived from a human colorectal carcinoma cell line (ACT no. CLL-247) were grown to 80–90% confluency in McCoy's 5A complete medium (Gibco catalog no. 16600-108) supplemented with 10% FBS and penicillin (100 U/mL)/streptomycin (100 µg/mL) and seeded at 4 × 10⁴ cells/well into prewarmed 96-well poly-D-lysine-coated plates and then incubated at 37 °C, 5% CO₂ for 4–6 h. At the end of the incubation period, nocodazole was added to the wells and maintained at a final concentration of 66 ng/mL to arrest the cells in mitosis. The cells were incubated with nocodazole overnight at 37 °C, 5% CO₂ for 16–18 h. At the end of the incubation period, the cells were added to a 96-well propylene plate containing compounds in DMSO that were serially diluted 3-fold down the row nine times for the generation of a nine-point curve. The cells were treated with compounds for 2 h at 37 °C, 5% CO₂. To harvest the HH3 protein, the medium was first aspirated from cells and the plate washed with cold PBS. The cells were lysed with cell extraction buffer (Biosource, catalog no. FNN0011) supplemented with phosphatase inhibitor (Roche catalog no. 11 83 580 001), and the plate was shaken at 5 °C for 30 min followed by centrifugation at 3000g for 20 min. The samples were then transferred to a Nunc PS 96-well plate and diluted in standard dilution buffer provided in the Path Scan phospho histone H3 (Ser 10) sandwich ELISA kit (Cell Signaling catalog no. 7155). The diluted samples were directly used following the protocol for the Path Scan phospho histone H3 (Ser 10) sandwich ELISA kit. The phosphorylation state of HH3 was detected using an anti-phospho-histone H3 (Ser10) antibody in a colorimetric sandwich ELISA. The reaction product was quantified by measuring the absorbance of the samples at 450 nm using a SpectraMax Plus 384 plate reader. The concentration of a compound that inhibited the phosphorylation of HH3 by 50% was reported as the pH3 IC₅₀ for that compound.

HTC-116 Cell Proliferation Assay. HCT-116 cells derived from a human colorectal carcinoma cell line (ATCC no. CCL-247) were grown to 50–70% confluency in McCoy's 5A complete medium (Gibco catalog no. 16600-108) with 10% FBS and penicillin (100 U/mL)/streptomycin (100 µg/mL). Cells were seeded at 800 cells/well in a 96-well plate and were allowed to incubate at 37 °C, 5% CO₂ overnight. On the following day, compounds in DMSO were serially diluted 3-fold down the row nine times for the generation of a nine-point curve. The diluted compounds were added to the plate containing cells and allowed to incubate for 72 h at 37 °C, 5% CO₂. At the end of the incubation period, the cells were directly used following the bromodeoxyuridine (BrdU) ELISA protocol described in the cell proliferation ELISA, BrdU (colorimetric) kit (catalog no. 11647229001, Roche Applied Science). The peroxidase reaction

product was quantified by measuring the absorbance of the samples at 450 and 690 nm using a SpectraMax Plus 384 plate reader. The concentration of a compound that inhibited the proliferation of HCT-116 by 50% was reported as the antiproliferation IC_{50} for that compound.

Pharmacokinetics. Precatheterized male SD rats (jugular vein, 230–300 g; Charles River, Hollister, CA) and female athymic Nu/Nu rat (tail vein, 225–250 g; Charles River, Hollister, CA) were acclimated in the vivarium for at least 3 days following delivery and prior to entering a study. Rats were fasted overnight before dosing. Compounds were administered iv to SD rats at 1 mg/kg in PEG400/water (3:1, v/v) and to Nu/Nu rats at 5, 15, and 50 mpk (compound **21c**) or 3, 10, and 30 mg/kg (compound **21i**) in Tween-80/PEG200/polyethylene glycol/water (2:10:5:83, v/v/v/v). Three rats were used per study arm. Blood was collected into K3 EDTA tubes at 5 min, 15 min, 30 min, 1 h, 2 h, 4 h, 6 h, and 24 h postdose. Collection tubes were mixed gently and spun at 4 °C to isolate the plasma. Plasma samples, calibration, and quality control standards (20 μ L) were extracted with six volumes of acetonitrile (ACN) containing an internal standard and analyzed by LC–MS/MS (Sciex 3200). Sample separation was achieved on a 5 μ m Zorbax SB-C8 column (4.6 mm \times 50 mm) using a 1.6 mL/min flow rate and a 1 min gradient (1.5 min cycle time) from 5% to 95% ACN containing 0.05% formic acid. The parent compound to fragment mass transitions of 582.1 \rightarrow 217.2 (**21c**) and 560.2 \rightarrow 195.3 (**21i**) were monitored. Peak areas were quantified using Analyst 1.4.1, and pharmacokinetic parameters were calculated from the normalized LC–MS/MS peak areas using a noncompartmental model and the linear trapezoidal estimation method with WinNonlin (Pharsight, version 5.2).

In Vivo Tumor Xenograft Studies. Female athymic nude rats (Nu/Nu Harlan Laboratories, Indianapolis, IN) between 8 and 9 weeks of age were implanted subcutaneously on day 0 with 5×10^6 HCT-116 cells in 200 μ L of PBS. Ten days later (designated as Day 1) rats were sorted into groups of 10 animals each with a mean tumor volume per group of 301–306 mm³. Both compounds **21c** and **21i** were formulated in TPPW and were administered by lateral tail vein injection. Each dose of the drug was delivered at a volume of 10 mL/kg and was adjusted for the body weight of the animal. Compound **21c** was given either at 5, 10, or 20 mg/kg on days 1, 3, 5, 8, 10, 12, 15, 17, 19 or at 2.5, 5, or 10 mg/kg on days 1–4, 8–11, 15–18. Compound **21i** was given at 10 or 20 mg/kg on days 1, 3, 5, 8, 10, 12, 15, 17, 19 and at 40 mg/kg on days 1, 3, 5, 8, and 10 and then at 30 mg/kg on days 15, 17, 19 because of a tolerability issue. An alternative schedule with compound **21i** was given at 5, 10, or 20 mg/kg on days 1–4, 8–11, 15–18. Camptosar (irinotecan) lot OAPWR was received as a commercial dosage formulation at 20 mg/mL in 5% dextrose in water (DSW). Animals were treated with Camptosar at 100 mg/kg ip qw \times 3. Animals with tumors in excess of 10 000 mg or with excessive ulcerated tumors were euthanized, as were those found in obvious distress or in a moribund condition. Body weights and tumor measurements were recorded twice weekly. Tumor burden was estimated from caliper measurements by the formula for the volume of a prolate ellipsoid, assuming unit density: tumor burden (mm³) = $(LW^2)/2$, where L and W are the respective orthogonal tumor length and width measurements in mm.

■ ASSOCIATED CONTENT

■ Supporting Information

Molecular modeling of a previously described Aurora inhibitor in complex with Aurora A; experimental data for compounds **2**, **5a–d,f,g**, **7b–e,g**, **21a,b,d–h,j–l**; complete list of additional kinase binding affinities determined for compounds **21c** and **21i**; additional nude rat xenograft efficacy figures for compounds **21c** and **21i**. This material is available free of charge via the Internet at <http://pubs.acs.org>.

■ AUTHOR INFORMATION

Corresponding Author

*Phone: 858-334-2164. Fax: 858-334-2192. E-mail: gliu@ambitbio.com.

Notes

The authors declare no competing financial interest.

■ ACKNOWLEDGMENTS

We thank Drs. Shripad S. Bhagwat and Wendell D. Wierenga for guidance and support. We thank the Ambit High Throughput Screening team (now a division of DiscoveRx) for kinase profiling and K_d measurements. We also thank Shanghai Syncores Technologies, Inc. for assistance in synthesizing some of the compounds listed herein. We also thank Piedmont Research Center, LLC for performing the nude rat xenograft studies.

■ ABBREVIATIONS USED

CAN, acetonitrile; pAURKA, phosphorylated Aurora A kinase; BrdU, bromodeoxyuridine; CL, clearance value; CR, complete regression; pHH3, histone H3 phosphorylation; QOD, every other day dosing; SD, Sprague–Dawley rat; TBTU, O-(benzotriazol-1-yl)-N,N,N',N'-tetramethyluronium tetrafluoroborate; TGI, tumor growth inhibition; TPPW, 2% Tween-80, 5% propylene glycol, 10% PG-400, 83% water

■ REFERENCES

- (1) Fu, J.; Bian, M.; Jiang, Q.; Zhang, C. Roles of Aurora Kinases in Mitosis and Tumorigenesis. *Mol. Cancer Res.* **2007**, *5*, 1–10.
- (2) (a) Rojanala, S.; Han, H.; Muñoz, R. M.; Browne, W.; Nagle, R.; VonHoff, D. D.; Bearss, D. J. The Mitotic Serine Threonine Kinase, Aurora-2, Is a Potential Target for Drug Development in Human Pancreatic Cancer. *Mol. Cancer Ther.* **2004**, *3*, 451–457. (b) Evans, R.; Naber, C.; Steffler, T.; Checkland, T.; Keats, J.; Maxwell, C.; Perry, T.; Chau, H.; Belch, A.; Pilarski, L.; Reiman, T. AuroraA Kinase RNAi and Small Molecule Inhibition of Aurora Kinases with VE-465 Induce Apoptotic Death in Multiple Myeloma Cells. *Leuk. Lymphoma* **2008**, *49*, S59–S69.
- (3) (a) Kallio, M. J.; McClelland, M. L.; Stukenberg, P. T.; Gorsky, G. J. Inhibition of Aurora B Kinase Blocks Chromosome Segregation, Overrides the Spindle Checkpoint, and Perturbs Microtubule Dynamics in Mitosis. *Curr. Biol.* **2002**, *12*, 900–905. (b) Harrington, E. A.; Bebbington, D.; Moore, J.; Rasmussen, R. K.; Ajose-Adeogun, A. O.; Nakayama, T.; Graham, J. A.; Demur, C.; Hercend, T.; Diu-Hercend, A.; Su, M.; Golec, J. M. C.; Miller, K. M. VX-680, a Potent and Selective Small-Molecule Inhibitor of the Aurora Kinases, Suppresses Tumor Growth in Vivo. *Nat. Med.* **2004**, *10*, 262–267.
- (4) Yang, H.; Burke, T.; Dempsey, J.; Diaz, B.; Collins, E.; Toth, J.; Beckmann, R.; Ye, X. Mitotic Requirement for Aurora A Kinase Is Bypassed in the Absence of Aurora B Kinase. *FEBS Lett.* **2005**, *579*, 3385–3391.
- (5) (a) Bischoff, J. R.; Anderson, L.; Zhu, Y.; Mossie, K.; Ng, L.; Souza, B.; Schryver, B.; Flanagan, P.; Clairvoyant, F.; Ginther, C.; Chan, C. S.; Novotny, M.; Slamon, D. J.; Plowman, G. D. A Homologue of Drosophila Aurora Kinase Is Oncogenic and Amplified in Human Colorectal Cancers. *EMBO J.* **1998**, *17*, 3052–3065. (b) Zeng, W. F.; Navaratne, K.; Prayson, R. A.; Weil, R. J.; Aurora, B. Expression Correlates with Aggressive Behaviour in Glioblastoma Multiforme. *J. Clin. Pathol.* **2007**, *60*, 218–221. (c) Naruganahalli, K. S.; Lakshmanan, M.; Dastidar, S. G.; Ray, A. Therapeutic Potential of Aurora Kinase Inhibitors in Cancer. *Curr. Opin. Invest. Drugs* **2006**, *7*, 1044–1051.
- (6) A number of comprehensive review articles have appeared in the literature: (a) Pollard, J. R.; Mortimore, M. Discovery and development of Aurora kinase inhibitors as anticancer agents. *J. Med.*

- Chem.* **2009**, *52*, 2629–2651. (b) Cheung, C.-H. A.; Coumar, M. S.; Hsieh, H.-P.; Chang, J.-Y. Aurora Kinase Inhibitors in Preclinical and Clinical Testing. *Expert Opin. Invest. Drugs* **2009**, *18*, 379–398.
- (7) Manfredi, M. G.; Ecsedy, J. A.; Meetze, K. A.; Balani, S. K.; Burenkova, O.; Chen, W.; Galvin, K. M.; Hoar, K. M.; Huck, J. J.; LeRoy, P. J.; Ray, E. T.; Sells, T. B.; Stringer, B.; Stroud, S. G.; Vos, T. J.; Weatherhead, G. S.; Wysong, D. R.; Zhang, M.; Bolen, J. B.; Claiborne, C. F. Antitumor Activity of MLN8054, an Orally Active Small-Molecule Inhibitor of Aurora A Kinase. *Proc. Natl. Acad. Sci. U.S.A.* **2007**, *104*, 4106–4111.
- (8) Mortlock, A. A.; Foote, K. M.; Heron, N. M.; Jung, F. H.; Pasquet, G.; Lohmann, J.-J. M.; Warin, N.; Renaud, F.; De Savi, C.; Roberts, N. J.; Johnson, T.; Dousson, C. B.; Hill, G. B.; Perkins, D.; Hatter, G.; Wilkinson, R. W.; Wedge, S. R.; Heaton, S. P.; Odedra, R.; Keen, N. J.; Crafter, C.; Brown, E.; Thompson, K.; Brightwell, S.; Khatri, L.; Brady, M. C.; Kearney, S.; McKillop, D.; Rhead, S.; Parry, T.; Green, S. Discovery, Synthesis, and in Vivo Activity of a New Class of Pyrazoloquinazolines as Selective Inhibitors of Aurora B Kinase. *J. Med. Chem.* **2007**, *50*, 2213–2224.
- (9) (a) Harrington, E. A.; Bebbington, D.; Moore, J.; Rasmussen, R. K.; Ajose-Adeogun, A. O.; Nakayama, T.; Graham, J. A.; Demur, C.; Hercend, T.; Diu-Hercend, A.; Su, M.; Golec, J. M. C.; Miller, K. M. VX-680, a Potent and Selective Small-Molecule Inhibitor of the Aurora Kinases, Suppresses Tumor Growth in Vivo. *Nat. Med.* **2004**, *10*, 262–267. (b) Giles, F. J.; Cortes, J. E.; Jones, D.; Bergstrom, D. A.; Kantarjian, H. M.; Freedman, S. J. MK-0457, a Novel Kinase Inhibitor, Is Active in Patients with Chronic Myeloid Leukemia or Acute Lymphocytic Leukemia with the T315I BCR-ABL Mutation. *Blood* **2007**, *109*, 500–502.
- (10) Carter, T. A.; Wodicka, L. M.; Shah, N. P.; Velasco, A. M.; Fabian, M. A.; Treiber, D. K.; Milanov, Z. V.; Atteridge, C. E.; Biggs, W. H.; Edeen, P. T.; Floyd, M.; Ford, J. M.; Grotzfeld, R. M.; Herrgard, S.; Insko, D. E.; Mehta, S. A.; Patel, H. K.; Pao, W.; Sawyers, C. L.; Varmus, H.; Zarrinkar, P. P.; Lockhart, D. J. Inhibition of Drug-Resistant Mutants of ABL, KIT, and EGF Receptor Kinases. *Proc. Natl. Acad. Sci. U.S.A.* **2005**, *102*, 11011–11016.
- (11) Abraham, S.; Hadd, M. J.; Tran, L.; Vickers, T.; Sidac, J.; Milanov, J.; Holladay, M. W.; Bhagwat, S. S.; Hua, H.; Ford Pulido, J. M.; Cramer, M. D.; Gitnick, D.; James, J.; Dao, A.; Belli, B.; Armstrong, R. C.; Treiber, D. K.; Liu, G. Novel Series of Pyrrolotriazine Analogs as Highly Potent Pan-Aurora Kinase Inhibitors. *Bioorg. Med. Chem. Lett.* **2011**, *21*, 5296–5300.
- (12) Abraham, S.; Bhagwat, S.; Hadd, M. J.; Holladay, M. W.; Liu, G.; Milanov, Z.; Patel, H.; Setti, E.; Sindac, J. A. Aurora Kinase Compounds and Methods of Their Use. WO2011/088045, July 21, 2011.
- (13) Fabian, M. A.; Biggs, W. H. III; Treiber, D. K.; Atteridge, C. E.; Azimioara, M. D.; Benedetti, M. G.; Carter, T. A.; Ciceri, P.; Edeen, P. T.; Floyd, M.; Ford, J. M.; Galvin, M.; Gerlack, J. L.; Grotzfeld, R. M.; Herrgard, S.; Insko, D. E.; Insko, M. A.; Lai, A. G.; Lelias, J.-M.; Mehta, S. A.; Milanov, Z. V.; Velasco, A. M.; Wodicka, L. M.; Patel, H. K.; Zarrinkar, P. P.; Lockhart, D. J. A Small Molecule–Kinase Interaction Map for Clinical Kinase Inhibitors. *Nat. Biotechnol.* **2005**, *23*, 329–336.
- (14) Carpinelli, P.; Moll, J. Aurora Kinase Inhibitors: Identification and Preclinical Validation of Their Biomarkers. *Expert Opin. Ther. Targets* **2008**, *12*, 69–80.
- (15) Karaman, M. W.; Herrgard, S.; Treiber, D. K.; Gallant, P.; Atteridge, C. E.; Campbell, B. T.; Chan, K. W.; Ciceri, P.; Davis, M. L.; Edeen, P. T.; Faraoni, R.; Floyd, M.; Hunt, J. P.; Lockhart, D. J.; Milanov, Z. V.; Morrison, M. J.; Pallares, G.; Patel, H. K.; Pritchard, L. M.; Wodicka, L. M.; Zarrinkar, P. P. A Quantitative Analysis of Kinase Inhibitor Selectivity. *Nat. Biotechnol.* **2008**, *26*, 127–132.
- (16) Additional information regarding KinomeScan, a division of DiscoveRx, is available at www.kinomescan.com.
- (17) Refer to the Supporting Information for details related to the molecular modeling of a previously described Aurora inhibitor in complex with Aurora A.
- (18) Treiber, D. K.; Lewis, W. G.; Wodicka, L. M. Cellular Assay Employing Detectable Protein. WO/2010/124157, 2010.
- (19) Kawasaki, A.; Matsumura, I.; Miyagawa, J.; Ezoe, S.; Tanaka, H.; Terada, Y.; Tatsuka, M.; Machii, T.; Miyazaki, H.; Furukawa, Y.; Kanakura, Y. Downregulation of an AIM-1 Kinase Couples with Megakaryocytic Polyploidization of Human Hematopoietic Cells. *J. Cell Biol.* **2001**, *152*, 275–287.
- (20) (a) Howard, S.; Berdini, V.; Boulstridge, J. A.; Carr, M. G.; Cross, D. M.; Curry, J.; Devine, L. A.; Early, T. R.; Fazal, L.; Gill, A. L.; Heathcote, M.; Maman, S.; Matthews, J. E.; McMenamin, R. L.; Navarro, E. F.; O'Brien, M. A.; O'Reilly, M.; Rees, D. C.; Reule, M.; Tisi, D.; Williams, G.; Vinkovic, M.; Wyatt, P. G. Fragment-Based Discovery of the Pyrazol-4-yl Urea (AT9283), a Multitargeted Kinase Inhibitor with Potent Aurora Kinase Activity. *J. Med. Chem.* **2009**, *52*, 379–388. (b) Arbitrario, J. P.; Belmont, B. J.; Evanchik, M. J.; Flanagan, W. M.; Fucini, R. V.; Hansen, S. K.; Harris, S. O.; Hashash, A.; Hoch, U.; Hogan, J. N.; Howlett, A. R.; Jacobs, J. W.; Lam, J. W.; Ritchie, S. C.; Romanowski, M. J.; Silverman, J. A.; Stockett, D. E.; Teague, J. N.; Zimmerman, K. M.; Taverna, P. SNS-314, a Pan-Aurora Kinase Inhibitor, Shows Potent Anti-tumor Activity and Dosing Flexibility in Vivo. *Cancer Chemother. Pharmacol.* **2009**, *65*, 707–717. (c) Hardwicke, M. A.; Oleykowski, C. A.; Plant, R.; Wang, J.; Liao, Q.; Moss, K.; Newlander, K.; Adams, J. L.; Dhanak, D.; Yang, J.; Lai, Z.; Sutton, D.; Patrick, D. GSK1070916, a Potent Aurora B/C Kinase Inhibitor with Broad Antitumor Activity in Tissue Culture Cells and Human Tumor Xenograft Models. *Mol. Cancer Ther.* **2009**, *8*, 1808–1817.
- (21) Marie-Christine Bissery, M.-C.; Guénard, D.; Guéritte-Voegelein, F.; Lavelle, F. Experimental Antitumor Activity of Taxotere (RP 56976, NSC 628503), a Taxol Analogue. *Cancer Res.* **1991**, *51*, 4845–4852.
- (22) The nude rat HCT-116 xenograft results for **21c** and **21i** from QD×4/week dosing schedule for 3 weeks can be found in the Supporting Information.
- (23) Refer to the Supporting Information for a complete list of kinases with K_d values determined for both compounds **21c** and **21i**.